

1 *Conference Proceedings Paper*

2 **Multifractal detrended fluctuation analysis of** 3 **relative humidity over Greece**

4 **Ioannis Koutsogiannis, Chris G. Tzani* and Anastasios Alimissis**

5 ¹ Climate and Climatic Change Group, Section of Environmental Physics and Meteorology, Department of
6 Physics, National and Kapodistrian University of Athens, 15784 Athens, Greece; koutsog@phys.uoa.gr (I.K.);
7 alimiss@phys.uoa.gr (A.A.)

8 * Correspondence: chtzani@phys.uoa.gr (C.G.T.)

9 Received: date; Accepted: date; Published: date

10 **Abstract:** Water, in its various forms, is considered a key parameter in climate change studies. Water
11 vapor is recognized as the most important natural greenhouse gas playing a vital role in the
12 hydrological cycle. Thus, studying air humidity fluctuations may contribute towards a deeper
13 understanding of the radiative and thermodynamic processes that take part in the Earth's
14 atmosphere. Traditional statistical analysis is not always efficient to describe complex physical
15 processes with high temporal variability. In addition, a more thorough study of the variations of
16 climatic parameters requires examination of their time series fluctuations over multiple time scales.
17 Fractal theory offers robust solutions that satisfy the above requirements. In this work, the
18 Multifractal Detrended Fluctuation Analysis (MF-DFA) is used in order to investigate the intrinsic
19 dynamics of daily relative humidity time series over the Greek region from a nonlinear perspective.
20 The scaling properties and the multifractal structure of the time series are studied by examining the
21 fluctuation function, the multifractal spectrum and the Hurst exponent.

22 **Keywords:** relative humidity; Multifractal Detrended Fluctuation Analysis; nonlinear dynamics;
23 climate change
24

25 **1. Introduction**

26 Meteorological time series are generally characterized by a nonlinear behavior. Therefore,
27 conventional statistical methods, which include the autocorrelation function or spectral analysis, are
28 not always capable of revealing the complex behavior of natural processes and parameters where
29 non-stationarities may exist. In addition, traditional statistical methods, such as trend analysis,
30 usually examine time series taking into account a single time scale and neglecting time series features
31 that occur over a wide range of temporal scales. The development of fractal theory has offered robust
32 solutions in order to overcome these issues. Fractal approaches, in general, are based on the division
33 of a time series into self-similar parts and the detection of the power-law behavior that reflects the
34 scaling characteristics of the system. Kantelhardt et al. [1] introduced the Multifractal Detrended
35 Fluctuation Analysis (MF-DFA) in order to determine the scaling behavior of time series with
36 statistical properties that vary temporally. It is widely considered a valuable tool for time series
37 analysis and has been used in a significant number of environmental studies [2-4]. Concerning the
38 Greek region, in particular, Kalamaras et al. [5-6] studied the multifractal characteristics of daily
39 temperature time series from meteorological stations of the Hellenic National Meteorological Service
40 network as well as their geographical distribution. Philippopoulos et al. [7] also investigated the
41 multifractal properties of daily temperature time series using the ERA-Interim reanalysis dataset.

42 Tzanis et al. [8] have also applied the Multifractal Detrended Cross-Correlation Analysis (MF-DCCA)
43 [9] in order to investigate the multifractal structure of the cross-correlation between global methane
44 and temperature. In this work, our scope is to study the multifractal characteristics and the scaling
45 behavior of daily relative humidity time series [10] from meteorological stations at different locations
46 within the Greek region.

47 2. Experiments

48 2.1 Data

49 Surface relative humidity (RH) observations during the synoptic hours (6, 12 and 18 UTC) were used
50 in this work. The RH data cover a complete 30-year period from 1975 to 2004 and were obtained from
51 three meteorological stations of the Hellenic National Meteorological Service (HNMS) network,
52 namely Thessaloniki, Athinai (Hellinikon), located in the city of Athens, and Herakleion (Figure 1).
53 The geographical characteristics of the three meteorological stations are summarized in Table 1. At
54 this point, it should be noted that significant data gaps exist after the selected time period and since
55 this work focuses only on the scaling properties of the time series the use of this data was avoided.
56 Prior to the application the MF-DFA method, the daily means (RH_{daily}) of the 6-hour relative humidity
57 data were calculated.

58

Table 1. List of meteorological stations

Station	WMO ID	Lat (N)	Lon (E)	Elev. a.s.l. (m)
Thessaloniki	16622	40° 31' 29"	22° 58' 18"	1.68
Athinai (Hellinikon)	16716	37° 53' 23"	23° 44' 31"	43.13
Herakleion	16754	35° 20' 07"	25° 10' 55"	39.00

59



60

61

Figure 1. Locations of meteorological stations under study

62 2.2 Methodology

63 The annual and semi-annual seasonal components that were identified in the daily relative humidity
64 time series were subsequently eliminated using the Wiener filter [11]. The MF-DFA methodology was
65 then applied to the time series of the deseasonalized surface RH data. A brief description of the MF-
66 DFA method is presented below:

67 1. The profile $X(i)$ is firstly constructed:

$$68 \quad X(i) = \sum_{k=1}^i [x_k - \langle x \rangle] \quad (1)$$

69 where by x_k and $\langle x \rangle$ the time series and its mean value are designated, respectively. The upper
70 bound of summation i takes values from 1 to N which corresponds to the length of the time series.

71 2. $X(i)$ is partitioned into an integer number of $N_s = \text{int}(N/s)$ non-intersecting segments all of which
72 have the same length s , i.e., time scale. The segmentation procedure is also repeated for the
73 retrograde time series of the profile. Thus, we get $2N_s$ segments in total.

74 3. Within each segment, a third-order ($m = 3$) polynomial \tilde{X}_v is fitted to the profile, representing
75 the local trend, where $v = 1, \dots, 2N_s$ is the number of each segment. The local trend is then
76 subtracted from the profile.

77 4. The detrended variance $F^2(s, v)$ is then calculated:

$$78 \quad F^2(s, v) = \left\{ \begin{array}{ll} \frac{1}{s} \sum_{i=1}^s \{X[(v-1)s+i] - \tilde{X}_v(i)\}^2, & \text{for } v = 1, \dots, N_s \\ \frac{1}{s} \sum_{i=1}^s \{X[(N-(v-N_s)s+i] - \tilde{X}_v(i)\}^2, & \text{for } v = N_s + 1, \dots, 2N_s \end{array} \right\} \quad (2)$$

79 5. Considering the average of all segments, we get the q^{th} order fluctuation function:

$$80 \quad F_q(s) = \left\{ \frac{1}{2N_s} \sum_{v=1}^{2N_s} [F^2(s, v)]^q \right\}^{\frac{1}{q}} \quad (3)$$

81 For $q = 0$ we have,

$$84 \quad F_0(s) = \exp \left(\frac{1}{4N_s} \sum_{v=1}^{2N_s} \ln[F^2(s, v)] \right) \quad (4)$$

82 $F_q(s)$ is determined only for $s \geq m+2$. For $q = 2$, the MF-DFA results are identical to the DFA procedure
83 [12-16].

85 6. $F_q(s)$ is computed for all values of s . The scaling behavior of $F_q(s)$ is examined through the plot of
86 $\log(F_q(s))$ against $\log(s)$ for each moment q . For time series which are long-range correlated, $F_q(s)$
87 follows a power law:

$$88 \quad F_q(s) \sim s^{h(q)} \quad (5)$$

89 For monofractal time series the scaling exponent $h(q)$ remains constant and it is equal to the Hurst
90 exponent H . For multifractal time series $h(q)$ depends strongly on q , i.e. the scaling behavior is
91 different for fluctuations of different magnitude. In these cases, $h(q)$ is the generalized form of the
92 Hurst exponent. For values of $h(q)$ between 0 and 0.5 the time series is characterized by long-range
93 negative correlation, denoting an anti-persistent character; for $h(q) > 0.5$, it is characterized by long-
94 range positive correlation (persistent behavior); for $h(q) = 0.5$ it is considered uncorrelated, i.e. white
95 noise.

96 Using the relationship $\tau(q)=qh(q)-1$ and applying a Legendre transformation we get

$$97 \quad \tau'(q) = \alpha \quad (6)$$

98 and

$$99 \quad f(\alpha) = q\alpha - \tau(q) = q[\alpha - h(q)] + 1 \quad (7)$$

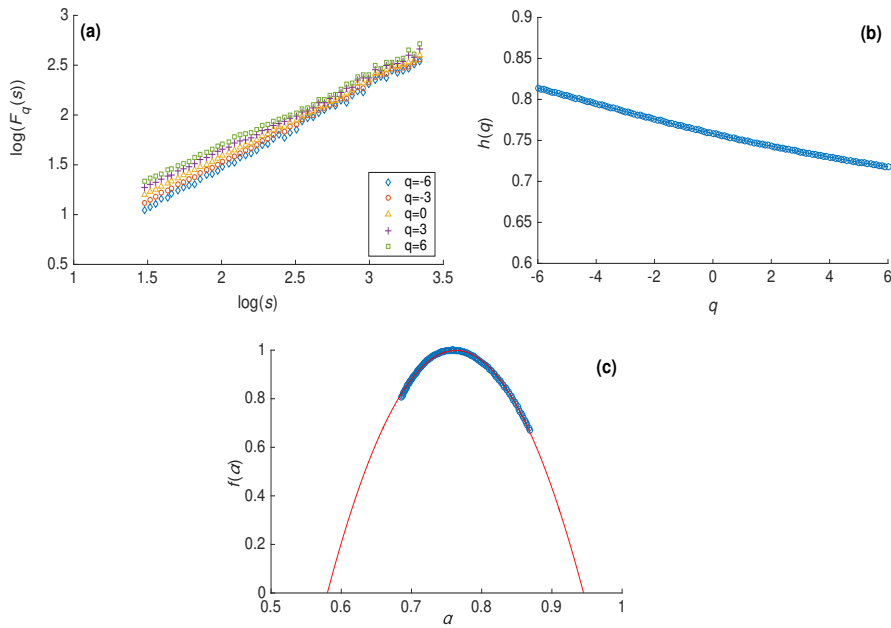
100 The plot of $f(\alpha)$ against α is the multifractal spectrum and gives information about the multifractal
101 structure of the time series. The value of α at which $f(\alpha)=\max$ is called the dominant Hurst exponent
102 α_0 and corresponds to the prevailing scaling behavior [17]. Along with α_0 , the spectral width w is also
103 a key feature. It can be estimated by fitting a second-order polynomial around α_0 as proposed by [18]
104 and measuring the distance between α_{max} and α_{min} , the two points where the fitting curve intersects
105 the horizontal axis:

$$106 \quad P(\alpha) = A(\alpha - \alpha_0)^2 + B(\alpha - \alpha_0) + C \quad (8)$$

107 A multifractal spectrum with a broad width indicates rich multifractality in the time series while
108 smaller widths are associated with a more monofractal character.

109 3. Results

110 After applying MF-DFA on the deseasonalized RH times series of the three meteorological
111 stations, the basic plots of the method are derived, namely a) the log-log plot of the fluctuation
112 function $F_q(s)$ against s , b) the plot of the generalized Hurst exponent $h(q)$ against the moments q and
113 c) the multifractal spectrum $f(\alpha)$ against α . In Figure 2 the plots concerning the meteorological station
114 of Thessaloniki are shown, however similar plots were obtained for the rest of the meteorological
115 stations as well. The time scales used in the MF-DFA process range between 30 months and $N/5$
116 where by N the length of the time series is denoted. The values of q also range from -6 to +6. From
117 examination of Figure 2 it can be observed that $\log(F_q(s))$ increases linearly with $\log(s)$ and the slopes
118 $h(q)$ are different for each q . This indicates that the relative humidity time series display multifractal
119 characteristics. In addition, $h(q)$ is greater than 0.5 for all moments q . From this, it can be deduced that
120 the time series of daily relative humidity are characterized by a persistent behavior (i.e. they are long-
121 range positively correlated). This indicates that past events exert an influence on the succeeding
122 values, i.e. an increase in the values of relative humidity is likely to be followed by an increase as
123 well.

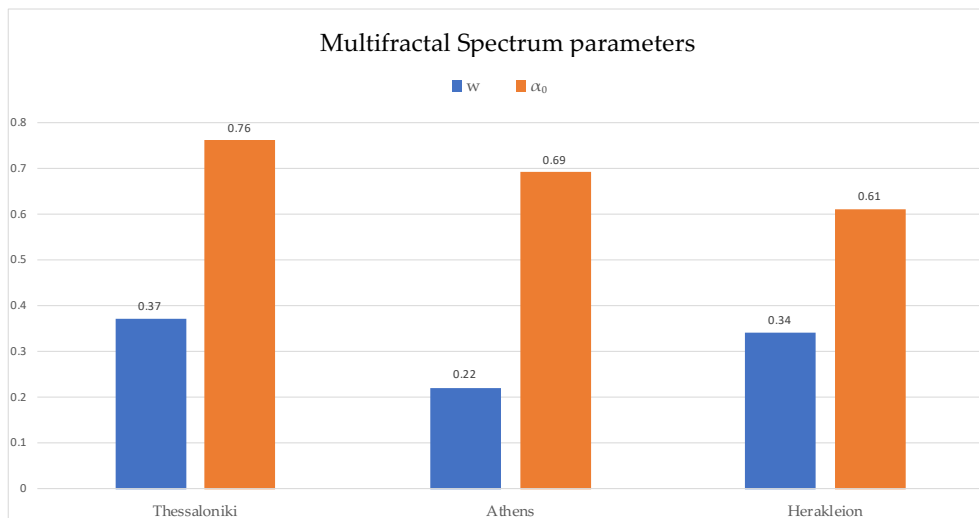


124

125 **Figure 2.** Multifractal Detrended Fluctuation Analysis (MF-DFA) results for RH from Thessaloniki
 126 station; **(a)** Plot of $\log(Fq(s))$ against $\log(s)$; **(b)** Plot of $h(q)$ against q ; and, **(c)** Multifractal spectrum
 127 $f(a)$ against a .

128 **4. Discussion**

129 Among the three stations examined, Thessaloniki demonstrates the highest value of α_0 , i.e. it
 130 exhibits the greatest persistence, while the lowest value was observed at Herakleion (Figure 3). This
 131 implies that the distribution of α_0 varies geographically with its values increasing with latitude. This
 132 could be attributed to the fact that the northern locations are more frequently influenced by
 133 atmospheric disturbances and the descent of dry cold air masses. This can cause significant
 134 temperature changes which may affect the persistence in the behavior of daily temperature time
 135 series. A decrease of daily temperature values leads to a decrease of the local atmosphere's water-
 136 holding capacity and thus an increase in daily relative humidity affecting also its persistence.
 137 Regarding the



138

139 **Figure 3.** Multifractal spectrum parameters (w, α_0) for the meteorological stations under study.

140

141 spectral width w , the stations of Thessaloniki and Herakleion exhibit similar values and thus a similar
142 degree of multifractality. On the other hand, the Athinai (Hellinikon) station presents a lower value
143 of w . This finding suggests that the time series of the meteorological station in Athens possesses
144 weaker multifractal features compared to the stations of Thessaloniki and Herakleion and therefore
145 they are characterized by a smaller degree of complexity. This could be attributed to the different
146 climatic conditions that prevail in the greater area of Athens.

147 5. Conclusions

148 In this work, daily relative humidity time series were examined for three meteorological stations at
149 different geographical regions of Greece using the MF-DFA method. The most interesting results can
150 be summarized as follows:

- 151 • Daily relative humidity time series are long-range positively correlated, which means that
152 an increase in the values of relative humidity is likely to be followed by an increase as
153 well.
- 154 • The values of the prevailing scaling exponent α_0 increase with increasing latitude. This
155 could be explained by temperature and thus relative humidity changes.
- 156 • Smaller values of spectral width w , and therefore weaker multifractality were found for
157 the meteorological station of Athinai (Hellinikon). This could be attributed to the different
158 climatic conditions that prevail in Athens.

159 **Author Contributions:** Conceptualization, I.K. and C.G.T.; methodology, I.K., C.G.T. and A.A.; software, I.K.,
160 C.G.T. and A.A.; validation, I.K., C.G.T. and A.A.; formal analysis, I.K., C.G.T. and A.A.; investigation, I.K.,
161 C.G.T. and A.A.; data curation, I.K., C.G.T. and A.A.; writing—original draft preparation, I.K., C.G.T. and A.A.;
162 writing—review and editing, I.K., C.G.T. and A.A.; visualization, I.K. and A.A.; supervision, C.G.T. All authors
163 have read and agreed to the published version of the manuscript.

164 **Funding:** This research received no external funding.

165 **Acknowledgments:** The authors would like to express their acknowledgements to the Hellenic National
166 Meteorological Service (HNMS) for providing the relative humidity data.

167 **Conflicts of Interest:** The authors declare no conflict of interest.

168 References

- 169 1. Kantelhardt, J.W.; Zschiegner, S.A.; Koscielny-Bunde, E.; Havlin, S.; Bunde, A.; Stanley, H.E.
170 Multifractal detrended fluctuation analysis of nonstationary time series. *Physica A* **2002**, *316*, 87–
171 114.
- 172 2. Du, H.; Wu, Z.; Zong, S.; Meng, X.; Wang, L. Assessing the characteristics of extreme precipitation
173 over northeast China using the multifractal detrended fluctuation analysis. *J. Geophys. Res. Atmos.*
174 **2013**, *118*, 6165–6174.
- 175 3. Zhou, Y.; Zhang, Q.; Singh, V.P. Fractal-based evaluation of the effect of water reservoirs on
176 hydrological processes: the dams in the Yangtze River as a case study. *Stoch. Env. Res. Risk A.*
177 **2014**, *28*, 263–279.

- 178 4. Baranowski, P.; Krzyszczak, J.; Slawinski, C.; Hoffmann, H.; Kozyra, J.; Nieróbca, A.; Siwek, K.;
179 Gluza, A. Multifractal analysis of meteorological time series to assess climate impacts. *Clim. Res.*
180 **2015**, *65*, 39–52.
- 181 5. Kalamaras, N.; Philippopoulos, K.; Deligiorgi, D.; Tzanis, C.G.; Karvounis, G. Multifractal scaling
182 properties of daily air temperature time series. *Chaos Soliton. Fract.* **2017**, *98*, 38–43.
- 183 6. Kalamaras, N.; Tzanis, C.G.; Deligiorgi, D.; Philippopoulos, K.; Koutsogiannis, I. Distribution of
184 air temperature multifractal characteristics over Greece. *Atmosphere* **2019**, *10*, 45.
- 185 7. Philippopoulos, K.; Kalamaras, N.; Tzanis, C.G.; Deligiorgi, D.; Koutsogiannis, I. Multifractal
186 Detrended Fluctuation Analysis of temperature reanalysis data over Greece. *Atmosphere* **2019**, *10*,
187 336.
- 188 8. Tzanis, C.G.; Koutsogiannis, I.; Philippopoulos, K.; Kalamaras, N. Multifractal Detrended Cross-
189 Correlation Analysis of Global Methane and Temperature. *Remote Sens.* **2020**, *12*, 557.
- 190 9. Zhou, W.-X. Multifractal detrended cross-correlation analysis for two nonstationary signals. *Phys.*
191 *Rev. E* **2008**, *77*, 066211.
- 192 10. Tzanis, C.G.; Koutsogiannis, I.; Philippopoulos, K.; Deligiorgi, D. Recent climate trends over
193 Greece. *Atmos. Res.* **2019**, *230*, 104623.
- 194 11. Wiener, N. *Extrapolation, Interpolation, and Smoothing of Stationary Time Series*; The MIT Press, 1949;
195 ISBN 9780262257190.
- 196 12. Varotsos, C.A.; Tzanis, C. A new tool for the study of the ozone hole dynamics over Antarctica.
197 *Atmos. Environ.* **2012**, *47*, 428–434.
- 198 13. Varotsos, C.A.; Lovejoy, S.; Sarlis, N. V.; Tzanis, C.G.; Efstathiou, M.N. On the scaling of the solar
199 incident flux. *Atmos. Chem. Phys.* **2015**, *15*, 7301–7306.
- 200 14. Efstathiou, M.N.; Tzanis, C.; Varotsos, C.A. Long-term memory dynamics of total ozone content.
201 *Int. J. Remote Sens.* **2009**, *30*, 3897–3905.
- 202 15. Varotsos, C.A.; Melnikova, I.; Efstathiou, M.N.; Tzanis, C. 1/f noise in the UV solar spectral
203 irradiance. *Theor. Appl. Climatol.* **2013**, *111*, 641–648.
- 204 16. Varotsos, C.A.; Milinevsky, G.; Grytsai, A.; Efstathiou, M.; Tzanis, C. Scaling effect in planetary
205 waves over Antarctica. *Int. J. Remote Sens.* **2008**, *29*, 2697–2704.
- 206 17. Bishop, S.M.; Yarham, S.I.; Navapurkar, V.U.; Menon, D.K.; Ercole, A. Multifractal Analysis of
207 Hemodynamic Behavior. *Anesthesiology* **2012**, *117*, 810–821.
- 208 18. Shimizu, Y.; Thurner, S.; Ehrenberger, K. Multifractal spectra as a measure of complexity in
209 human posture. *Fractals* **2002**, *10*, 103–116.



© 2020 by the authors. Submitted for possible open access publication under the terms and conditions of the Creative Commons Attribution (CC BY) license (<http://creativecommons.org/licenses/by/4.0/>).